Peer-reviewed version available at Genes 2017, 8, 61; doi:10.3390/genes8020061

Article

In Vivo Imaging of Local Gene Expression Induced by Magnetic Hyperthermia

Olivier Sandre [1,*], Coralie Genevois [2], Eneko Garaio [3], Laurent Adumeau [4], Stéphane Mornet [4] and Franck Couillaud [2,*]

1 Laboratoire de Chimie des Polymères Organiques, LCPO, UMR 5629 CNRS, University Bordeaux, 33076 Bordeaux-INP, Pessac, France
2 Imagerie Moléculaire et Thérapies Innovantes en Oncologie, IMOTION, EA 7435, University Bordeaux, 33076 Bordeaux, France; coralie.genevois@u-bordeaux.fr
3 Elektrizitatea eta Elektronika Saila, UPV/EHU, P.K. 644, Bilbao, Spain; eneko.garayo@ehu.eus,
4 CNRS, University Bordeaux, ICMCB, UPR 9048, F-33600 Pessac, France; laurent.adumeau@gmail.com (L.A.); stephane.mornet@icmcb.cnrs.fr (S.M.)
* Correspondence: olivier.sandre@enscbp.fr (O.S.); franck.couillaud@u-bordeaux.fr (F.C.)

Abstract: The present work aims to demonstrate that colloidal dispersions of magnetic iron oxide nanoparticles stabilized with dextran macromolecules placed in an alternating magnetic field can not only produce heat, but also that these particles could be used *in vivo* for local and non-invasive deposition of a thermal dose sufficient to trigger thermo-induced gene expression. Iron oxide nanoparticles were first characterized *in vitro* on a bio-inspired setup, and then they were assayed *in vivo* using a transgenic mouse strain expressing the luciferase reporter gene under transcriptional control of a thermosensitive promoter. Iron oxide nanoparticles dispersions were applied topically on the mouse skin or injected sub-cutaneously with Matrigel™ to generate so called pseudo tumors. Temperature was monitored continuously with a feedback loop to control the power of the magnetic field generator and to avoid overheating. Thermo-induced luciferase expression was followed by bioluminescence imaging 6 hours after heating. We showed that dextran-coated magnetic iron oxide nanoparticles dispersions were able to induce *in vivo* mild hyperthermia compatible with thermo-induced gene expression in surrounding tissues and without impairing cell viability. These data open new therapeutic perspectives for using mild magnetic hyperthermia as non-invasive modulation of tumor microenvironment by local thermo-induced gene expression or drug release.

Keywords: magnetic hyperthermia; gene therapies; heat shock protein promoter; *in vivo* optical imaging; magnetic polymer-coated nanoparticles

1. Introduction

Gene therapies are promising techniques for curing diseases either by repairing or replacing a defective gene or by expressing some therapeutic proteins or regulatory non coding RNA. In spite of some well-known successes such as therapy of cross-linked severe combined immunodeficiency (X-SCID) [1] and quite a lot of clinical trials [2], gene therapies are not widely used in clinical practices. Safe, specific and efficient delivery of a therapeutic gene to an identified cell or organ still remains an important challenge but efficient control of transgene expression also requires considerable improvement.

Tight spatiotemporal regulation of gene expression in the region where therapy is necessary and for the duration required to achieve a therapeutic effect is very important for clinical applications of gene therapy and to minimize systemic toxicity. Temporal control of gene expression may be achieved by several externally controlled, inducible gene promoters which respond to antibiotics [3] and other small molecules [4]. Spatial control is more frequently envisaged by using tissue-specific or disease-specific promoters yet lacking features for both temporal and external

controls. Furthermore, these specific promoters often exhibit a low level of therapeutic gene expression.

Hyperthermia in combination with temperature sensitive heat shock protein (Hsp70) promoter presents a unique approach allowing non-invasive spatiotemporal control of transgene expression. We already demonstrated *in vivo* by using transgenic mice and genetically modified cells that focused ultrasound (FUS) combined with real-time monitoring of the local temperature distribution by phase magnetic resonance imaging allows for a fine control of temperature increase and thus a good spatiotemporal control of local transgene expression by using thermosensitive promoters [5–7].

Magneto-activable thermogenic nanoparticles (MTN) as heat sources also appeared as an attractive alternative especially for deep-seated and poorly accessible tumors [8,9]. MTN injection into tumors and their subsequent heating using an alternating magnetic field has been developed as a cancer treatment for several decades and after a phase II clinical trial at the end of 2011, it was authorized against severe brain cancer (glioblastoma) in combination with conventional radiotherapy and is currently proposed as a clinical tool. Depending on the temperature increase and the duration, tumor cell killing or increased susceptibility to concomitant radio- or chemotherapy has been observed [8–10]. MTN-based hyperthermia treatment also increases tumor sensitivity to natural killer cell mediated lysis [11] and tumor-specific immune responses resulting from thermo-induction of heat-shock proteins (Hsp) expression [12,13].

The present paper aims to demonstrate that MTNs could be used *in vivo* for local and non-invasive deposition of sufficient thermal dose to trigger transgene expression by thermosensitive promoter. Chosen MTNs are colloidal dispersions of magnetic iron oxide nanoparticles stabilized with dextran macromolecules. We first establish MTN heating properties on a bio-inspired *in vitro* setup, and then we move on a thermosensitive transgenic mouse strain already characterized *in vivo* by bioluminescence imaging for its response to mild-hyperthermia [14,15].

2. Materials and Methods

2.1. Animals and animals handling

Animal experiments were performed in agreement with European directives and approved by the local ethical comity (CEEA 50) under agreement A50120195. The double transgenic mouse Hspa1b-lucF (+/+) Hspa1b-mPlum (+/+)[15] was housed at the University of Bordeaux facilities and maintained under 12 hours light/dark cycle with water and food *ad libitum*. Animals were anesthetized with 2% isoflurane (Belamont, Nicholas Piramal Limited, London, UK) in air. Prior experiments, mice were shaved with clippers and a depilatory cream.

2.2. MTN synthesis and characterization

Magnetic nanoparticles (MNPs) synthesized by various chemical routes are studied for their potential use in medicine, in particular for magnetic hyperthermia [16,17]. In this work, MNPs were synthesized by alkaline co-precipitation of ferrous and ferric salts followed by size sorting procedure as previously described [18]. Briefly, magnetite (Fe_3O_4) MNPs right after the co-precipitation reaction were totally oxidized into maghemite (γ-Fe_2O_3) by boiling ferric nitrate[19] and dispersed in dilute nitric acid. Then they were submitted to a size-sorting procedure based on the liquid–liquid phase-separation obtained by screening the electrostatic repulsions with an excess of electrolyte (HNO_3) concentration, yet below 0.4 M (pH>0.4) in order to prevent MNP dissolution into ions. The principle of this sorting is that the concentrated phase is enriched with the larger NPs, whereas the dilute phase contains the smaller MNPs [18,20,21]. After repeating several phase separation and washing steps (three cycles), the sample named C1C2C3 originated from the concentrated phase fractions corresponding to the concentrated phases obtained by adding HNO_3 electrolyte to the preceding pelleted fractions. The ions in excess were washed off with acetone and diethyl ether, resulting into a suspension in diluted HNO_3 at pH ~ 2 and at an iron oxide concentration of 110 g/L. These particles displayed a mean nanoparticle size of 12.4 nm (with standard deviation σ = 6.0 nm), as measured by automated particle counting on a TEM image (Supplementary materials). This 'ionic

ferrofluid' was then coated by dextran T70 (Mw 70 kDa, Sigma-Aldrich, Saint-Quentin Fallavier, France) in order to be dispersible in aqueous buffer at neutral pH and also in a protein hydrogel matrix (called hereinafter Matrigel™). For this coating, a volume of 5 mL of ferrofluid at 110 g/L was added to 30 mL of dextran solution at 100 g/L and then let to incubate overnight under gentle shaking. This dispersion was precipitated in 120 mL of ethanol and particles were separated magnetically from free (un-adsorbed) dextran macromolecular chains. This dextran precipitation not only allows to remove most of the polymer excess but also to promote the adhesion of glucose monomers onto the nanoparticle surface through hydrogen bonds. The pellet was dispersed in 40 mL of sterile ultrapure water (18 MΩ·cm) produced by using a SG-Labostar (7 TWF-UV system from Odemi, Grisy, France) and heated at 70°C under vacuum in order to remove residual ethanol. Finally, free dextran chains were removed by several washes (2 times with a dilution factor of about 10) with ultrapure water by tangential flow filtration (TFF) using 300 kDa cutoff ultra-filtration filters (Merck Millipore). At the end of the procedure, these magnetic nanoparticles contain 15.4 % of dextran determined by TGA analysis (data shown as supporting information). Finally, the so-prepared ferrofluid thereafter denominated C1C2C3@dex was concentrated by TFF in phosphate buffer saline (PBS) to obtain an iron oxide concentration of 117 g/L as measured by a UV-Vis spectrum (Supplementary materials). Their hydrodynamic diameter was measured by dynamic light scattering (DLS) after 200 times dilution in water with a Malvern™ NanoZS apparatus operating at 90° scattering angle, giving a Z-average diameter of 40.2 nm with low polydispersity (PDI=0.215). Their specific heating power was characterized by the 'specific absorption rate' in the alternating magnetic field (AMF) conditions used (H=10.2 kA/m at 755 kHz). A value SAR=94±1 W/g was found from the initial slope of the temperature profile within the first 3 sec of AMF application (supporting information). In previous work containing extensive magnetic characterization, we showed that this sample has a SAR verifying the linear response theory based on Néel and Brown relaxation processes of the magnetic moments, using independent magnetic measurements of the specific magnetization and of the magnetic anisotropy constant [18].

2.3. In vitro MTN experiments (phantoms)

An aliquot of C1C2C3@dex nanoparticles (20, 25, 30 or 35 µL), diluted to 50 µL with water, was mixed with 50 µL of Matrigel™ (BD Matrigel™ Basement Membrane Matrix ; Becton, Dickinson and Company, San José, CA, USA) at temperature near 4°C. Previously, it was checked that Matrigel™ diluted twice still jellified when raising temperature to 37°C. The mixture was poured into a cell culture insert (24 wells; ø pores: 0.8 µm) and covered by an agar plug (Figure 1B). The insert was placed into an agar gel (20 mL; 2 % w/v) modeling the heat capacity of a mouse (body weight around 20 g) which was placed in a thermostatic double-wall chamber (Figure 1A). The system was then placed in the middle of the solenoid and maintained at 37 °C (Figure 1C) by the water circuit linked to a regulating bath (Huber Polystat CC, Offenburg, Germany) before the alternating magnetic field (AMF) was generated by the coil. An optical fiber thermo-probe (OTG-M420; Opsens™ Inc, Québec, Canada) was introduced inside the insert through a catheter (20 G, TERUMO®) to reach the C1C2C3@dex nanoparticle/Matrigel™ mixture.

2.4. In vivo MTN experiments (animals)

MTNs were diluted in water and applied topically on the mouse skin. Diluted MTNs were also mixed with Matrigel™ at 4°C and injected sub-cutaneously on the back of the mouse to generate so called 'pseudo-tumor'. After 30 min, the Matrigel™ was gelled and the mouse was placed inside the solenoid. Optical fiber thermo-probe (OTG-M420; Opsens™, Québec, QC, Canada) was inserted into the pseudo-tumor using a Teflon™ catheter (20 G, TERUMO®) as guide. Room temperature around the coil was monitored during the experiment and maintained at 20°C.

2.5. Hyperthermia setup and protocol

The electric generator (SEIT ELECTRONICA, Junior™ 3.5 kW model creates an alternating magnetic field (AMF) inside a 4-turn copper-ring solenoid of 55 mm outer diameter, 48 mm inner diameter and 38 mm height. The solenoid is refrigerated by a cold (18°C) water flux inside the 3.5 mm diameter, 0.4 mm wall thick, hollow wires of the solenoid. Magnetic field intensity is H=10.2 kA/m, induction B=12.8 mT and frequency 755 kHz as determined by finite element modelling for magnetics (FEMM, http://www.femm.info), after measuring the high voltage (747 V) and deducing the current (234 Amps) from the calculated coil impedance (R= 3.2 Ω) and inductance (L=4.5×10^{-9} H). The field value calculated by finite element modelling was also checked experimentally by measuring the electromotive force in a scout coil (1 turn of 17.5 mm diameter): 29.4 V peak to peak.

Homemade software was developed in LabVIEW™ allowing temperature regulation during the heating process according to predefined parameters i.e. duration (in seconds), maximum temperature and thermal dose above a threshold temperature. The thermal dose is defined as the integral of the temperature vs. time profile above a predetermined threshold, usually 42°C. This definition is equivalent to the 'equivalent total time at 43°C' expressed in 'degree-minute' (tdm_{43}) [22].

2.6. In vivo bioluminescence imaging (BLI)

BLI was performed at the Vivoptic platform (Bordeaux University & CNRS, UMS 3767) using a NightOWL II LB 983 calibrated system equipped with a NC 100 CCD deep-cooled camera (Berthold Technologies™, Bad Wildbad, Germany). Mice were injected intraperitoneally with D-luciferin (2.9 mg in 100 µL PBS, Promega™, Madison, Wisconsin, USA,) and sedated 5 min later. Bioluminescence images (1 min exposure, 4×4 binning) and photographs (100 ms exposure) were taken 8 min after the luciferin injection. A low light emitting standard (Glowell, LUX biotechnology™, UK) was placed next to the animal during each image acquisition to provide a quality control. Pseudo-color images representing the spatial distribution of emitted photons were generated using IndiGO 2 software (Berthold Technologies™) and superposed to the corresponding photographs.

3. Results

3.1. Heating performances of MTN in vitro on bio-inspired phantom.

We first assayed MTN heating performances using an *in vitro* bio-inspired setup. MTN were mixed with Matrigel™, a natural component of the tumor microenvironment placed into a 20 mL agar gel to mimic a mouse weight of about 20 g. The tumor phantom model was designed with a volume of 100 µL in order to exceed the diameter of 1.1 mm proposed by Rabin as a minimum size of magnetic sample to exhibit macroscopic heating compared to environmental temperature[23]. The agar gel was actively thermo-regulated at 37 °C using a water flux. MTNs were mixed with Matrigel™ at final iron oxide concentration of 23.4, 35.1 and 40.8 g/L. The maximum temperature that can be reached in Matrigel™ phantoms depends on their volume and on the concentration of their contained MTNs. Figure 1D shows the temperature profiles obtained for the maximum power of the generator providing magnetic field intensity of B= 12.8 mT at 755 kHz. The temperature initially at 37 °C rapidly increases and reaches a plateau that is maintained as long as the magnetic field is maintained, corresponding to perfect balance between the heat flux created by the MTNs and the thermal losses at the interface between the magnetic phantom and the surrounding hydrogel mimicking the mouse body. Activation was repeated several times in order to check the reproducibility of the bio-mimic system. Observation of the MTN-containing Matrigel™ after the experiment reveals a poor homogeneity of the spatial distribution of MTNs for an iron oxide concentration of 40.95 g/L. At a concentration of 35.1 g/L, the maximum temperature obtained is 48 °C while MTNs are homogeneously distributed in the Matrigel™ tumor phantom.

Preprints (www.preprints.org) | NOT PEER-REVIEWED | Posted: 24 January 2017 doi:10.20944/preprints201701.0105.v1

Peer-reviewed version available at Genes 2017, 8, 61; doi:10.3390/genes8020061

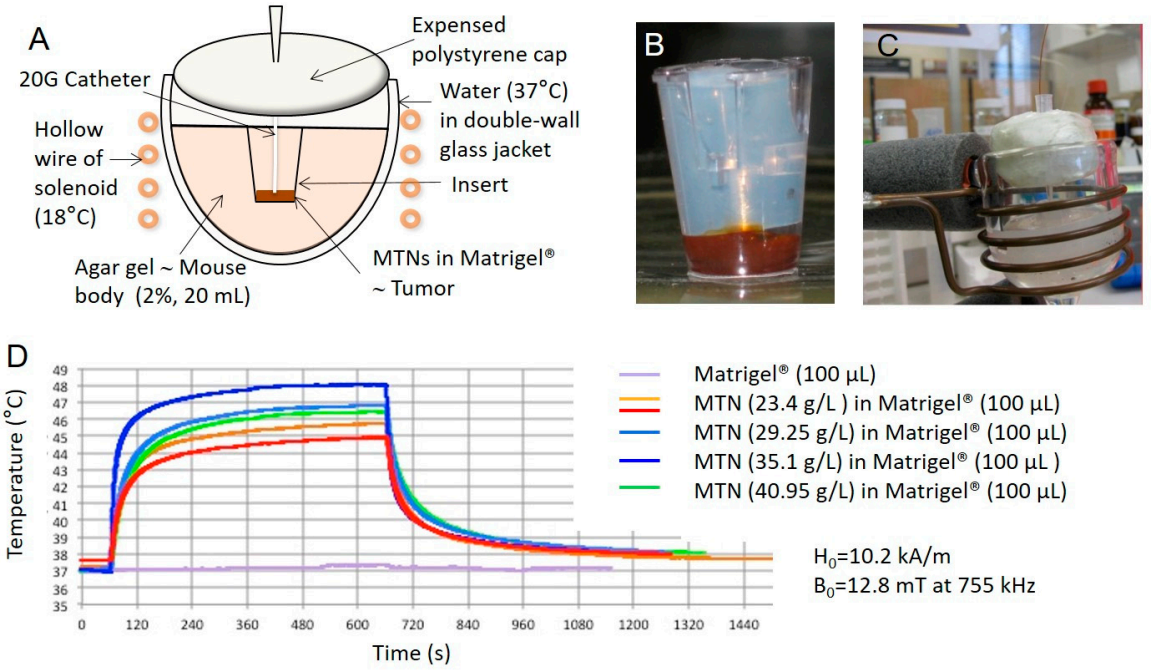

Figure 1. Heating performances of MTNs in a bio-inspired phantom. (A) Schematic representation of the experimental setup. Phantoms were made of 100 µL Matrigel™ containing MTNs at different concentrations and poured into a cell culture insert (24 wells; ø pores: 0.8 µm) to mimic a tumor (B). Insert was covered by an agar plug and inserted into a 20 mL agar gel (2 % w/v) of thermal inertia equivalent to the mouse body. (C) Phantom was placed into a thermostatic chamber maintained at 37°C through water circulation within double-walled glass water jacket to represent "active" thermal regulation by the mouse blood circulation, and located in the middle of the solenoid. The complete system reached thermal equilibrium at 37 °C before the alternating magnetic field was generated. An optical fiber thermal probe (Opsens® OTG-M420) was introduced into the insert up to reaching the MTN/Matrigel™ mixture through a catheter (20 G, TERUMO®). (D) Time courses of temperature in the magnetic field of induction *B*=12.8 mT at 755 kHz (*H*=10.2 kA/m) according to different MTN concentrations.

3.2. In silico modeling of temperature distribution in the bio-inspired phantom.

Numerical modeling of thermal distribution was used to predict MTN heating upon activation. The finite element software FEMM can perform numerical simulations not only of magnetics but also of the Fourier heat diffusion and convection equation. The grid model took into account all parameters of the experimental device including dimensions of the various compartments, fixed temperature (37°C) at the boundary of the glass jacket with convective conditions, and thermal characteristics of the Matrigel™ and agar media such as heat capacity and conductivity, taken as pure water values (C_P=4.18 J/cm³/K, k=0.6 W/m/K). Figure 2 shows the modeling results for MTN concentration of 35 g/L in the 100 µL Matrigel™ phantom. The iron oxide mass in the phantom (3.5 mg) can irradiate a power $3.5\times10^{-3}\times94$=0.33 W in a 100 µL volume, thus a power density of 3.3 W/cm³. A somehow lower estimated value p=2 W/cm³ was taken in the simulation to take into account the decrease of SAR when the MNPs are partially blocked within the gel matrix as compared to the homogeneous fluid (Brown relaxation mechanism is likely impeded). This 40% decrease of SAR is arbitrary, but it is quite in line with a systematic study of the local concentration negative effect on SAR for similar hydrophilic polymer-coated MTNs [24]. The maximum temperature is predicted in the center of Matrigel™ insert and temperature gradually decreases with distance from the center. The temperature difference is nearly 10 ° C between the Matrigel™ center and the border of the agar block containing the insert, yet with variation between 45°C and 47°C depending on the axial and lateral coordinates. The temperature predicted by the numerical model in the center rose to 48.5 °C,

which is very close to the experimental value of 48°C reported in Figure 1D for the same concentration (35 g/L). However, these curves show non-monotonous variation with concentration in the experiments, which might be ascribed to Matrigel™ heterogeneity or unprecise localization of the optical fiber temperature probe (in agreement with the thermal gradient calculated numerically).

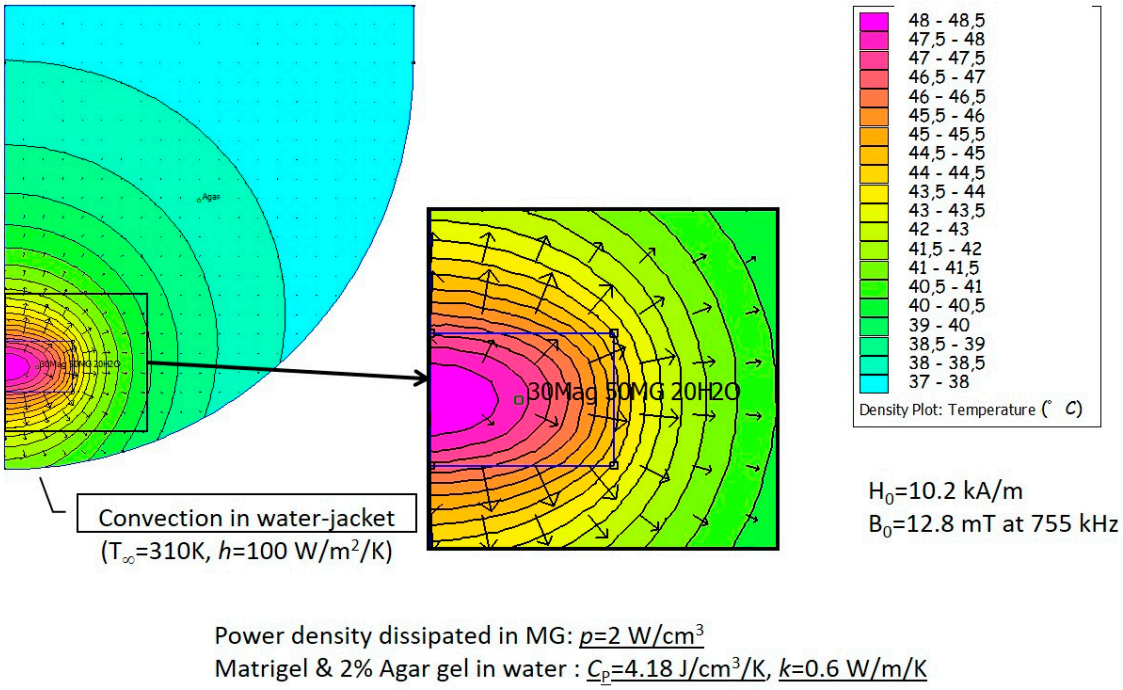

Figure 2. Numerical modelling of thermal distribution in the Matrigel™ phantom with 3709 nodes using FEMM freeware (http://www.femm.info/). The power density was chosen to correspond to a MTN concentration of 35.1 g/L under an alternating magnetic field *B*=12.8 mT at 755 kHz (*H*=10.2 kA/m). At thermal equilibrium (stationary state of the heat equation), maximal temperatures of 48°C in the center of the Matrigel™ insert and of 44°C at the insert periphery were predicted by the numerical model.

3.3. Topical application of MTN solution on transgenic mouse skin

MTN aqueous suspension (69 g/L, 100 µL) was applied on the skin of Hsp70-lucF transgenic mouse. Mouse was placed in the middle of the solenoid and an optical fiber thermo-probe was immersed in the MTN fluid droplet (Figure 3A). Temperature was monitored using LabView™ home-made program to drive the generator and thus the magnetic field created by the solenoid (Figure 3B). The magnetic field generator was switched off when the temperature inside the MTN drop reached 45°C and was switched on again at 44 °C, leading to a saw-tooth temperature profile. Applied magnetic field was *B*=12.8 mT at 755 kHz (*H*=10.2 kA/m). As shown in Figure 3C, heating was maintained for 10 min until the AMF was definitively switched off, temperature decreasing rapidly to the baseline skin temperature (32°C). BLI measurement was performed 6 hours after magnetic heating according to previous data reporting HSP-dependent lucF expression [15]. Figure 3D illustrates hsp-dependent lucF expression as revealed by BLI. As controls, MTNs were applied on the mouse skin without magnetic field or when mouse was placed into the magnetic field for 10 min without MTNs, and then no BLI signal was detected (data not shown).

Preprints (www.preprints.org) | NOT PEER-REVIEWED | Posted: 24 January 2017 doi:10.20944/preprints201701.0105.v1

Peer-reviewed version available at Genes 2017, 8, 61; doi:10.3390/genes8020061

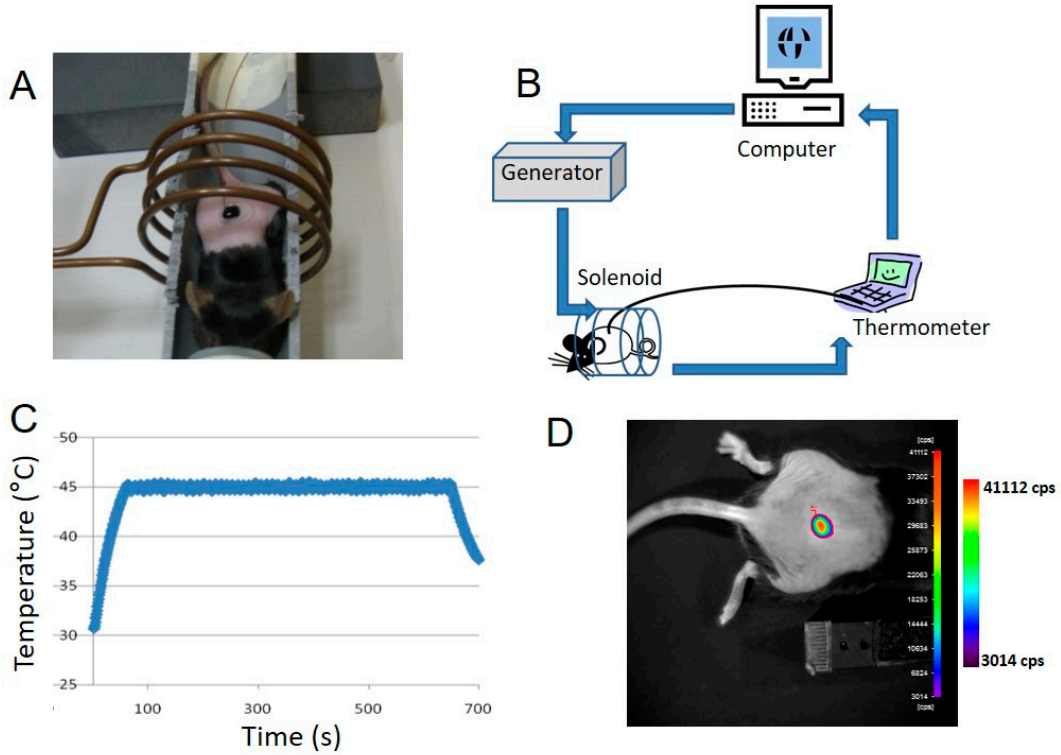

Figure 3. Imaging of heat-induced expression of luciferase by magnetic activation of MTN applied on the transgenic mouse skin. (A) An MTN drop (69 g/L, 100 µL water) was applied on Hsp70-lucF transgenic mouse skin. Mouse was placed on a bed aligned with the central axis of the solenoid. An optical fiber thermo-probe was immersed in the MTN droplet. (B) On/off cycles of alternating magnetic field (B=12.8 mT at 755 kHz (H=10.2 kA/m)) were created by a computer-controlled generator according to the temperature recorded in the drop (T_{on}=44°C, T_{off}=45°C). (C) Examples of temperature measurements in the MTN solution. (D) Bioluminescence imaging of thermo-induced luciferase expression by the mouse skin, 6 hours after magnetic hyperthermia.

3.4. Subcutaneous MTN-containing Matrigel™ pseudo-tumors in mice

To test MTN induced intratumoral hyperthermia with further realism towards therapeutic application, Matrigel™ pseudo-tumors containing MTNs (35.1 g/L) were created subcutaneously in Hsp/LucF transgenic mice by injection of the mixture in the cold fluid state. A Teflon™ catheter was introduced into the pseudo-tumors to be used as a guide for the fiber optics temperature probe. Temperature was monitored using software developed under LabView™ to drive the generator and thus the magnetic field inside the solenoid. Maximum temperature was fixed at 45°C and running time was defined according to calculation of the predefined thermal dose expressed as tdm_{43} (i.e. time interval equivalent to a thermal dose calculated above a threshold temperature of 42°C). As shown on figure 4, magnetic activation of Matrigel™ pseudo-tumors containing MTNs heating results into lucF expression by mouse tissues as detected by BLI 6 hours after heating. Different types of BLI pattern were obtained. Some mice exhibited “Gaussian type” BLI pattern (figure 4A; n=5) whereas some other exhibited “ring shape” BLI patterns with no BLI signal in the middle of the heated zone (Figure 4 B; n=13). The pattern was not related to the predefined thermal dose as illustrated on Figure 4.

Preprints (www.preprints.org) | NOT PEER-REVIEWED | Posted: 24 January 2017 doi:10.20944/preprints201701.0105.v1

Peer-reviewed version available at Genes 2017, 8, 61; doi:10.3390/genes8020061

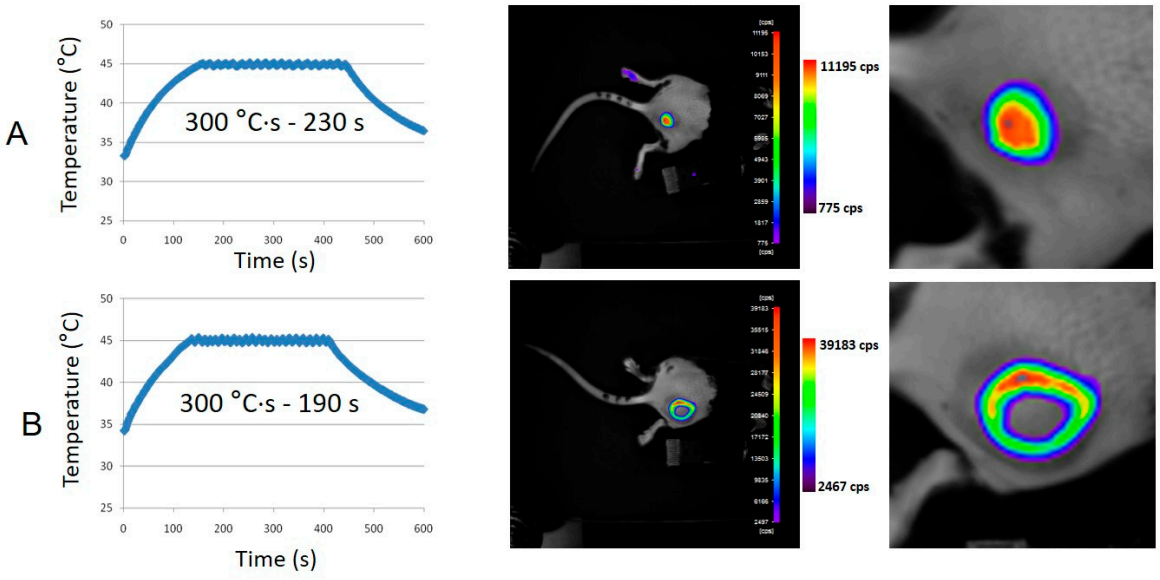

Figure 4. Imaging of heat-induced expression of luciferase by magnetic activation of Matrigel™ pseudo-tumors containing MTNs. Cold Matrigel™ (50 µL) added to MTNs (30 µL at 115 g/L, 20 µL water) leading to 100 µL at 34.5 g/L final MTN concentration were injected subcutaneously and allowed to solidify for 30 min at mouse body temperature. Mouse is placed in the middle of the solenoid. An optical fibre thermo-probe (360 µm) was inserted in the Matrigel™ volume using a Teflon™ catheter. Magnetic field (B=12.8 mT at 755 kHz (H=10.2 kA/m)) is created by a PC-controlled generator (on/off cycles) according to temperature recorded in the Matrigel™ volume. Predefined thermal dose was 300 °C·s calculated above 42°C, or an equivalent time at 43°C tdm_{43}=5 min, and upper limit temperature was set at 45°C. Line A and B are BLI images of thermo-induced luciferase expression by the mouse tissues, 6 hours after magnetic hyperthermia.

Soaking the leg of the transgenic mice in warm water (45 °C, 8 min) induces HSP promoter activation and LucF expression, as detected by BLI 6 hours later [14,15]. To determine the physiological status of the central area of the ring shape pattern, the mouse paw was immersed in a water bath (45 °C, 8 min, tdm_{43}=24 min). Six hours after this heating, the whole paw expresses luciferase except the central area of the ring. This lack of signal therefore corresponds to an area where cells have lost the ability to express luciferase. Transgenic mice with Matrigel™ pseudo-tumors containing MTNs without AMF application or with Matrigel™ pseudo-tumors alone and placed in the AMF did not exhibit BLI signal. Mice bearing pseudo-tumors with MTN concentration lower than 35 g/L did not exhibit BLI signal (11 g/L, 15 min AMF on; 15 g/L 15 min AMF on; 18 g/L 15 min AMF on; n=5; data not shown).

3.5. In silico modeling of temperature distribution in MTN-containing pseudo-tumors

Using the same finite element modeling FEMM software than used for bioinspired phantoms, temperature mapping in MTN-containing Matrigel™ pseudo-tumors was assayed upon activation with different tumor shapes that can arise after subcutaneous injection of a given volume of 100 µL. Thermal characteristics of the different tissues were obtained from the literature [25]. Figure 5 shows the modeling results for MTN concentration of 35 g/L in 100 µL Matrigel™ pseudo-tumors located below the skin. According to the pseudo-tumor shape, the estimated temperature on the skin surface facing the BLI camera increased from 46.2 °C (flat disk-like tumor) up to 57.2°C (cylindrical tumor of larger thickness, thus lower surface area and less thermal losses towards the surrounding tissues).

Preprints (www.preprints.org) | NOT PEER-REVIEWED | Posted: 24 January 2017 doi:10.20944/preprints201701.0105.v1

Peer-reviewed version available at Genes 2017, 8, 61; doi:10.3390/genes8020061

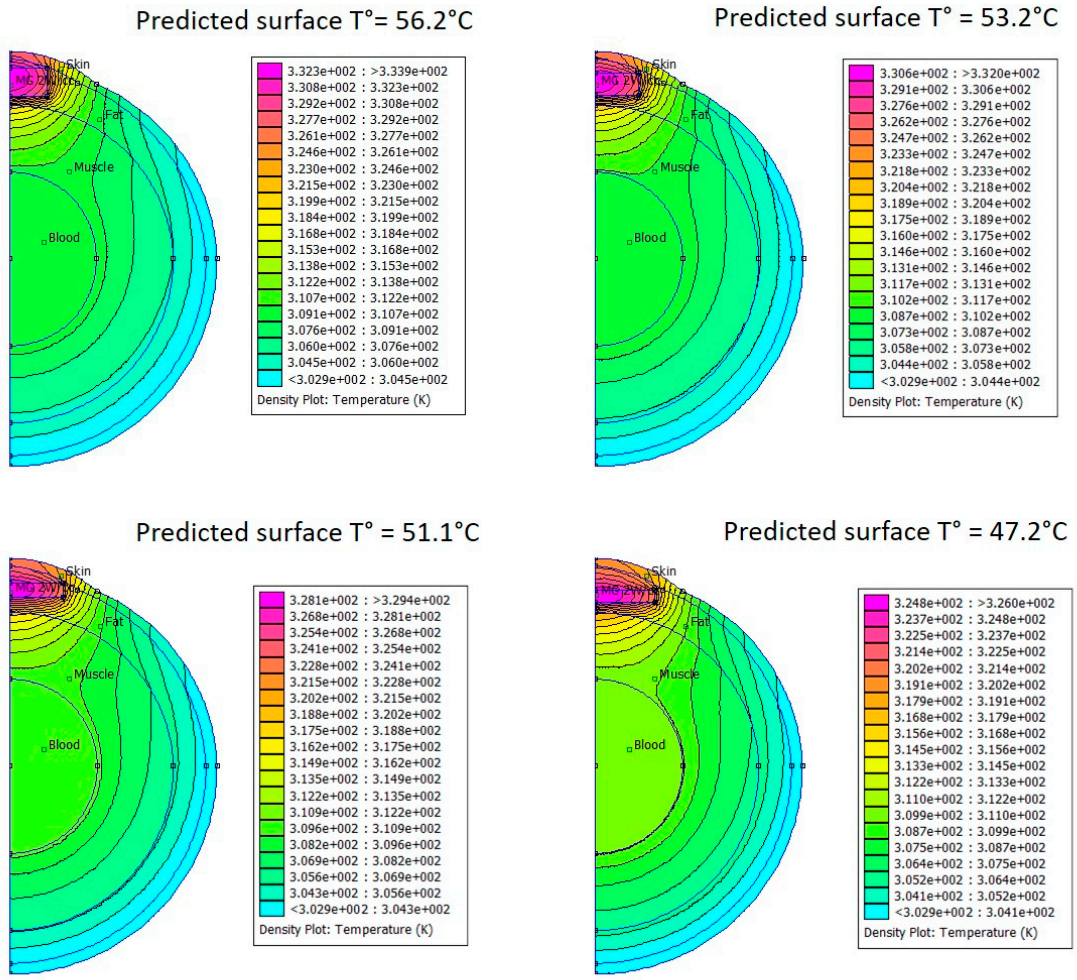

Figure 5. Numerical modeling (FEMM grid with ~7800 nodes) of temperature spatial distribution in and around a subcutaneous pseudo-tumor placed in the fat layer (3 mm thick) below skin (1 mm) and above muscles for different tumor shapes at constant 100 µL volume. Blood volume is 2.1 mL. MTN are supposed to dissipate a heat power density p=2 W/cm^3 under an alternating magnetic field was B=12.8 mT at 755 kHz (H=10.2 kA/m). Thermal parameters (heat capacity and conductivity) used are taken from literature:[22] (C_P=3.28 J/cm^3/K; k=0.37 W/m/K) for skin, (C_P=1.93 J/cm^3/K; k=0.16 W/m/K) for fat, (C_P=3.87 J/cm^3/K; k=0.48 W/m/K) for muscle, (C_P=4.18 J/cm^3/K; k=0.6 W/m/K) for blood pool, supposed isothermal at T_0=310K. Predicted temperatures at the pseudo-tumor surface were 56.2, 53.2, 51.1 and 47.2 °C according to pseudo-tumor cylindrical shape heights of 2.6, 2, 1.34, and 1.04 mm respectively (for same 100 µL volume).

4. Discussion

In the present paper, we demonstrate the feasibility of inducing gene expression *in vivo* by magnetic hyperthermia. When MTNs were placed in an alternating magnetic field, they produced heat which dissipated into the surrounding environment. The challenge was to use MTN-based heating in physiological environment and to generate enough thermal energy to activate the thermosensitive promoter in cells of surrounding tissues. The transgenic mouse used is expressing the reporter gene lucF under transcriptional control of the hsp70 thermosensitive promoter, and this mouse has been already fully characterized for its response to mild hyperthermia [14]. For temperature above 43°C, temperature-induced Hsp70 promoter activation was modulated by both temperature as well as duration of hyperthermia and the reporter gene expression can be modelled by an Arrhenius analysis [14]. Typically, by soaking mouse paw in a water bath at 45°C for 8 min

(calculated thermal dose =1440 °C·s above 42°C thus tmd_{43}=24 min), a high BLI signal was expressed by skin [14,15]. The calculated average activation energy required for activation of Hsp70 promoter in this mouse was 559 kJ/mol leading to a K-factor of about 2, indicating that for temperature above 43°C, an increase in temperature of 1 °C is equivalent to decreasing the exposure time with a factor 2 [14]. The light emission after heating attests for both HSP promoter activation and cell viability. The BLI readout requires indeed lucF translation and both oxygen and ATP-dependent lucF enzymatic activity.

To mimic the thermic conditions in mouse exposed to magnetic hyperthermia, we reported at first a phantom system consisting in a 20 mL soft aqueous gel with a peripheral water circulating system thermalized at 37 °C representing blood circulation. To mimic a tumor stroma, a MTN droplet was diluted to 100 µL with water and Matrigel™, which is a commercially available natural component of the extracellular matrix. In this medium, the state of dispersion of MTNs is believed to be closed to mouse extracellular medium (i.e. there are partially blocked in the water pocket of the tight network. The upper concentration of MTNs in Matrigel™ without impeding the gel formation is limited to about 35 g/L, which constituted a first limitation. Higher concentration results in MTN precipitation in Matrigel™ and impairs heating performance. As a second limitation, we found that in such conditions, heating capacity of MTNs is limited, lowered by a factor around 40% (as estimated to the heat power density p=2 W/cm^3 necessary for according experiments and thermic simulations, as compared to p=3.3 W/cm^3 calculated from the SAR in liquid state). At a temperature of 37°C, Matrigel™ indeed forms a dense protein network of 50-500 nm mesh-size [26], in which the polysaccharide-coated magnetic NPs presumably are adsorbed and blocked, hampering the Brown relaxation mechanism of their magnetic moment under an AMF. When Matrigel™ pseudo-tumors containing MTNs (35 g/L) were placed in the alternative magnetic field, the temperature rose and rapidly reached a plateau at about 48 °C in the magnetic field conditions used. Lower concentrations of MTNs resulted in lower plateau temperatures, and thus the lower limit of 43 °C required to induce cellular heat stress was not reached [27].

Application of MTNs in aqueous liquid droplets on the mouse skin and subsequent activation by alternating magnetic field resulted in significant temperature increase, despite heat dissipation in air. To prevent any hazard and extensive tissues damage, the temperature was recorded continuously and limited to 45 °C. Such protocol ensures thermal dose calculation in real time and allowed for lucF expression. Although not as extensively studied in the present work as needed for a quantitative relationship, the BLI signal was well correlated with the thermal dose deposited on the mouse skin defined as the integral of time-temperature curve above 42°C with a coefficient of determination R^2=0.999 (n=3: linear fit in Supporting Information) and was consistent with previously reported data using warm water as heating source.

MTNs diluted in cold liquid Matrigel™ at 35 g/L and injected subcutaneously in mouse formed a solid mass when reaching physiological temperature of the animal. Placing the mouse into the alternating magnetic field resulted in MTN activation. The main result of this work was to evidence that magnetically induced heat generation was sufficient to induce HSP-dependent transgene expression in surrounding tissues. The temperature was recorded continuously by placing a thermal probe inside the Matrigel™ mass: Although the position of the 420 µm fiber in the mm-sized tumor phantom was not sufficiently precise to guarantee to be in the exact geometrical center of the pseudo-tumor, the temperature rise could be limited by software control of the AMF generation to 45 °C. However, certainly due to this imprecision of probe localization, BLI patterns of transgene activation appeared very variable and not well correlated to the recorded thermal dose. In particular, ring shape BLI patterns with a no light emitting area in the middle were observed in some cases. Ring shape activation patterns have been already reported and were resulting to local overheating resulting in central tissues necrosis and Hsp activation at periphery [6]. This suggest that the recorded temperature was not representative of the overall temperature rise in the Matrigel™ mass and that thermal probe may be not located in the warmer point of the Matrigel™ pseudo-tumor volume, but rather at its periphery, explaining the underestimation of the recorded temperature (and hence overheating and cell catabolism in the central part).

Peer-reviewed version available at Genes 2017, 8, 61; doi:10.3390/genes8020061

Modeling thermal exchanges by finite element modelling (FEM) simulation of the heat equation with biologically relevant parameters provided good correlation between simulations and experimental measurements. It is indeed the case when applied to the phantom setup that provided consistent prediction of the maximum temperature reached at thermal equilibrium (i.e. when generated heat is balanced by thermal losses). For *in vivo* experiment using MTNs dispersed in Matrigel™, numerical modelling clearly illustrated that the temperature field is not homogeneous in the Matrigel™ volume. The higher temperature was calculated in the geometrical center of the Matrigel™ volume, and the predicted temperature profiles exhibited a centrifuge gradient. *In vivo*, perfect positioning of the thermal probe in the center of the Matrigel™ could not be precisely achieved nor checked. Incorrect positioning provided false evaluation of the overall temperature in the Matrigel™ and further mistaking of the feedback loop software controlling the magnetic field. This may explain in part the ring BLI patterns ascribed to overheating and catabolism/necrosis of the cells in contact with the hottest spots. Modeling also illustrated changes in thermal profiles according to pseudo-tumor shapes. MTN/Matrigel™ mixtures were injected in fluid state and solidify in various shapes ranging from "almost spherical" to "flat disk". Modeling prediction revealed up to 9 °C of difference between expected temperatures on pseudo-tumor surface according to the different shapes, as ascribed to different surface-to-volume ratio and thus thermal losses in surrounding matrix, resulting in huge differences in the thermal dose delivered to tissues.

The HSP70 promoter is activated not only by heat stress but also in response to a variety of stresses of both environmental and physiological origins [28]. Stressors include oxidative stress [29], toxic compounds [28], hypoxia, ischemia, acidosis, energy depletion, cytokines and UV radiation [30]. In the current study, no BLI signal was detected after MTN topical application or MTN pseudo tumor injection in absence of magnetic field-activation. It is also pointed that only female mice were used for the study to avoid BLI resulting from mechanical stresses and resulting scar ascribed to fight between males. In literature, it has been shown that intracellular magnetic field-activated MTN can activate Hsp70 response *in vitro* [13] or induce toxicity on targeted cancer cells without a detectable temperature rise [10]. Intracellular internalization of MTNs is not expected to occur in our current experiments as MTN suspension was deposited on skin for a very short time or the MTNs were embedded in Matrigel™. Activation of HSP response without consistent temperature rise was not observed. For instance, when recorded temperature did not reach temperature above 43 °C or the thermal dose required for heat-induced Hsp70 activation by using lower MTN concentration in Matrigel™ pseudo tumors or shorter activation times, no BLI signal was detected. In other words, a macroscopic temperature rise was necessary to induce HSP gene expression in this *in vivo* study.

The current work clearly revealed current practical limitations of the MTN-based strategy for controlling gene expression. As stated above, concentrations of the MTN required for HSP promoter activation is very high, close to the limit of dispersability of the magnetic NPs in biological media. More efficient magnetic NPs (exhibiting higher SAR) may be relevant to develop for future studies. Difficulties also occurred in controlling MTN homogeneity, which induced variations in the temperature field distribution. Finally, the major limitation is due to inadequate methods for temperature control *in vivo* and for determination of MTN distribution within the tumor microenvironment, resulting in unexpected events such as over-heating. Possible amelioration could be to perform magnetic resonance imaging of the pseudo-tumor right before the AMF application, in order to check the exact position of the catheter and the fiber optics temperature probe.

In conclusion, we showed that polysaccharide-coated maghemite nanoparticles either deposited on the skin or injected into subcutaneous tumor phantoms were able to induce *in vivo* mild hyperthermia compatible with thermo-induced gene expression in surrounding tissues, without impairing cell viability. Although limitations still remain for finer temperature measurement and limitation, and thus, control of transgene expression, these data opened new therapeutic perspectives for using mild magnetic hyperthermia for non-invasive modulation of tumor microenvironment by local thermo-induced gene expression or local drug release.

Acknowledgments We thank Pauline Durand for technical assistance, Pierre Costet and Laetitia Medan (Univ. Bordeaux) for animal breading and care. This work was supported by Emerging program of Cancéropôle Grand Sud-Ouest and 'Défi Nano' 2014 program from CNRS Interdisciplinary Mission. Authors also thank COST Action RADIOMAG (TD1402), supported by COST (European Cooperation in Science and Technology). O.S. thanks the Agence Nationale de la Recherche (grant ANR-13-BS08-0017 MagnetoChemoBlast). Work was done within LabEx TRAIL (ANR-10-LABX-57) community and the imaging Platform was supported by France Life Imaging.

Conflicts of Interests, The authors declare no conflict of interest

References

1. Cavazzana-Calvo, M.; Hacein-Bey, S.; de Saint Basile, G.; Gross, F.; Yvon, E.; Nusbaum, P.; Selz, F.; Hue, C.; Certain, S.; Casanova, J. L.; Bousso, P.; Deist, F. L.; Fischer, A. Gene therapy of human severe combined immunodeficiency (SCID)-X1 disease. *Science* **2000**, *288*, 669–672.

2. Edelstein, M. L.; Abedi, M. R.; Wixon, J. Gene therapy clinical trials worldwide to 2007--an update. *J. Gene Med.* **2007**, *9*, 833–842.

3. Iida, A.; Chen, S. T.; Friedmann, T.; Yee, J. K. Inducible gene expression by retrovirus-mediated transfer of a modified tetracycline-regulated system. *J. Virol.* **1996**, *70*, 6054–6059.

4. Clackson, T. Controlling mammalian gene expression with small molecules. *Curr. Opin. Chem. Biol.* **1997**, *1*, 210–218.

5. Deckers, R.; Quesson, B.; Arsaut, J.; Eimer, S.; Couillaud, F.; Moonen, C. T. Image-guided, noninvasive, spatiotemporal control of gene expression. *Proc Natl Acad Sci U A* **2009**, *106*, 1175–80.

6. Eker, O. F.; Quesson, B.; Rome, C.; Arsaut, J.; Deminière, C.; Moonen, C. T.; Grenier, N.; Couillaud, F. Combination of cell delivery and thermoinducible transcription for in vivo spatiotemporal control of gene expression: a feasibility study. *Radiology* **2011**, *258*, 496–504.

7. Fortin, P.-Y.; Lepetit-Coiffé, M.; Genevois, C.; Debeissat, C.; Quesson, B.; Moonen, C. T. W.; Konsman, J. P.; Couillaud, F. Spatiotemporal control of gene expression in bone-marrow derived cells of the tumor microenvironment induced by MRI guided focused ultrasound. *Oncotarget* **2015**, *6*, 23417–23426.

8. Thiesen, B.; Jordan, A. Clinical applications of magnetic nanoparticles for hyperthermia. *Int. J. Hyperth. Off. J. Eur. Soc. Hyperthermic Oncol. North Am. Hyperth. Group* **2008**, *24*, 467–474.

9. Kobayashi, T. Cancer hyperthermia using magnetic nanoparticles. *Biotechnol. J.* **2011**, *6*, 1342–1347.

10. Creixell, M.; Bohórquez, A. C.; Torres-Lugo, M.; Rinaldi, C. EGFR-targeted magnetic nanoparticle heaters kill cancer cells without a perceptible temperature rise. *ACS Nano* **2011**, *5*, 7124–7129.

11. Kubista, B.; Trieb, K.; Blahovec, H.; Kotz, R.; Micksche, M. Hyperthermia increases the susceptibility of chondro- and osteosarcoma cells to natural killer cell-mediated lysis. *Anticancer Res.* **2002**, *22*, 789–792.

12. Ito, A.; Matsuoka, F.; Honda, H.; Kobayashi, T. Antitumor effects of combined therapy of recombinant heat shock protein 70 and hyperthermia using magnetic nanoparticles in an experimental subcutaneous murine melanoma. *Cancer Immunol. Immunother.* **2004**, *53*, 26–32.

13. Moros, M.; Ambrosone, A.; Stepien, G.; Fabozzi, F.; Marchesano, V.; Castaldi, A.; Tino, A.; de la Fuente, J. M.; Tortiglione, C. Deciphering intracellular events triggered by mild magnetic hyperthermia in vitro and in vivo. *Nanomed.* **2015**, *10*, 2167–2183.

14. Deckers, R.; Debeissat, C.; Fortin, P.-Y.; Moonen, C. T. W.; Couillaud, F. Arrhenius analysis of the relationship between hyperthermia and Hsp70 promoter activation: A comparison between ex vivo and in vivo data. *Int. J. Hyperth. Off. J. Eur. Soc. Hyperthermic Oncol. North Am. Hyperth. Group* **2012**, *28*, 441–450.

15. Fortin, P.-Y.; Genevois, C.; Chapolard, M.; Santalucía, T.; Planas, A. M.; Couillaud, F. Dual-reporter in vivo imaging of transient and inducible heat-shock promoter activation. *Biomed. Opt. Express* **2014**, *5*, 457–467.

16. Périgo, E. A.; Hemery, G.; Sandre, O.; Ortega, D.; Garaio, E.; Plazaola, F.; Teran, F. J. Fundamentals and advances in magnetic hyperthermia. *Appl. Phys. Rev.* **2015**, *2*, 41302.

17. Duguet, E.; Vasseur, S.; Mornet, S.; Devoisselle, J.-M. Magnetic nanoparticles and their applications in medicine. *Nanomed.* **2006**, *1*, 157–168.

18. Garaio, E.; Sandre, O.; Collantes, J.-M.; Garcia, J. A.; Mornet, S.; Plazaola, F. Specific absorption rate dependence on temperature in magnetic field hyperthermia measured by dynamic hysteresis losses (ac magnetometry). *Nanotechnology* **2015**, *26*, 15704.

19. Tourinho, F. A.; Franck, R.; Massart, R. Aqueous ferrofluids based on manganese and cobalt ferrites. *J. Mater. Sci.* **1990**, *25*, 3249–3254.

20. Massart, R.; Dubois, E.; Cabuil, V.; Hasmonay, E. Preparation and properties of monodisperse magnetic fluids. *J. Magn. Magn. Mater.* **1995**, *149*, 1–5.

21. Arosio, P.; Thévenot, J.; Orlando, T.; Orsini, F.; Corti, M.; Mariani, M.; Bordonali, L.; Innocenti, C.; Sangregorio, C.; Oliveira, H.; Lecommandoux, S.; Lascialfari, A.; Sandre, O. Hybrid iron oxide-copolymer micelles and vesicles as contrast agents for MRI: impact of the nanostructure on the relaxometric properties. *J. Mater. Chem. B* **2013**, *1*, 5317–5328.

22. Sapareto, S. A.; Dewey, W. C. Thermal dose determination in cancer therapy. *Int. J. Radiat. Oncol. Biol. Phys.* **1984**, *10*, 787–800.

23. Rabin, Y. Is intracellular hyperthermia superior to extracellular hyperthermia in the thermal sense? *Int. J. Hyperthermia* **2002**, *18*, 194–202.

24. Piñeiro-Redondo, Y.; Bañobre-López, M.; Pardiñas-Blanco, I.; Goya, G.; López-Quintela, M. A.; Rivas, J. The influence of colloidal parameters on the specific power absorption of PAA-coated magnetite nanoparticles. *Nanoscale Res. Lett.* **2011**, *6*, 383.

25. Levy, A.; Dayan, A.; Ben-David, M.; Gannot, I. A new thermography-based approach to early detection of cancer utilizing magnetic nanoparticles theory simulation and in vitro validation. *Nanomedicine Nanotechnol. Biol. Med.* **2010**, *6*, 786–796.

26. Poincloux, R.; Lizárraga, F.; Chavrier, P. Matrix invasion by tumour cells: a focus on MT1-MMP trafficking to invadopodia. *J. Cell Sci.* **2009**, *122*, 3015–3024.

27. van Rhoon, G. C.; Samaras, T.; Yarmolenko, P. S.; Dewhirst, M. W.; Neufeld, E.; Kuster, N. CEM43°C thermal dose thresholds: a potential guide for magnetic resonance radiofrequency exposure levels? *Eur. Radiol.* **2013**, *23*, 2215–2227.

28. Morimoto, R. I. Cells in stress: transcriptional activation of heat shock genes. *Science* **1993**, *259*, 1409–1410.

29. Freeman, M. L.; Borrelli, M. J.; Syed, K.; Senisterra, G.; Stafford, D. M.; Lepock, J. R. Characterization of a signal generated by oxidation of protein thiols that activates the heat shock transcription factor. *J. Cell. Physiol.* **1995**, *164*, 356–366.

30. Kregel, K. C. Heat shock proteins: modifying factors in physiological stress responses and acquired thermotolerance. *J. Appl. Physiol. Bethesda Md 1985* **2002**, *92*, 2177–2186.